ISSN 1330-3651 (Print), ISSN 1848-6339 (Online)
https://doi.org/10.17559/TV-20230210000344
Original scientific paper

Split Ring Resonator Inspired Dual-Band Monopole Antenna for ISM, WLAN, WIFI, and WiMAX Application

Roja GANESAN, Maheswara Venkatesh PANCHAVARNAM*, Jayasankar THANGAIYAN

Abstract: A dual-band antenna is used for several wireless networks like ISM, WLAN, WiMAX, and WiFi. The antenna's uppermost element is a monopole shape with a rectangular protrusion. Antennas are created in CST. Using a 19-millimetre-wide by 31-millimetre-long FR4 substrate, the antenna is created in a design environment. Due to the SRR printing in the ground and the antenna's defective ground structure, the antenna is able to achieve dual resonance. A split ring resonator printed at the base also helps achieve a second resonance. With the help of a parameter analysis, we can pick the optimal proportions for the design. The antenna resonates at both 2.3 and 5.8 GHz. We construct and test the antenna. The results obtained through simulation are equivalent to those obtained from measurements in terms of s11, gain, and directivity, as well as E-plane and H-plane patterns. Because of its compact size, consistent radiation pattern, dual-band use, and excellent impedance matching and bandwidth, the suggested antenna is an excellent choice for use in ISM networks and other wireless applications.

Keywords: dual-band; metamaterial; SRR; WiMAX; WLAN

1 INTRODUCTION

The design of a miniaturized antenna with enough bandwidth capacity is the major difficulty in today's compact portable communication devices, which are integrated with modern wireless communication systems like Bluetooth, WIFI, WLAN, WiMAX, etc. [1, 2]. Because of its small size, low cost, and ease of etching on a single FR4 substrate, the monopole antenna is ideal under these circumstances. The literature has a number of designs aimed at wireless applications. Our goal is to create an antenna with enough bandwidth for WLAN/WiMAX applications. Numerous methods for enhancing bandwidth are described in the literature, including the use of metasurfaces as a superstrate [3], bioelectric loading [4], metamaterial [5], the addition of ground strips and slits [6], the inclusion of ZOR as a parasitic element [7, 11], the CPs impedance Tuner [8], the LC resonator [9], and fractal architectures [10]. All the above methods are capable of increasing the bandwidth, but the major drawback is that it makes the antenna design more complex, and it also has a direct effect on the radiation pattern.

Negative permittivity and permeability materials are not frequently seen in nature. These characteristics are produced by the structure of the object rather than by its components. The metamaterial is the name for those kinds of electromagnetic structures. The remarkable electromagnetic properties of metamaterials are positively influencing the propagation direction of electromagnetic waves. The design of antenna [12, 13], filters [14-16], communication equipment [15, 16], and couplers [16] can all be done using metamaterials. The metamaterials are artificial electromagnetic structures with Pg/4-sized unit cells that behave like actual materials and have well-defined sequential characteristics [17]. Researchers are very interested in using metamaterials to improve antenna performance because of their distinctive electromagnetic activity. Some types of metamaterials include the Split Ring Resonator (SRR) [18], Omega-shaped [19], and Complementary Split Ring Resonator (CSRR) [20-23]. These materials are used for size reduction, bandwidth enhancement, and impedance matching. The SRR's quasi-static resonant characteristic [24-26] allows for the construction of highly compact antennas with a wavelength much shorter than its physical dimensions, which have a very low gain.

This work presents a monopole microstrip antenna for WLAN/WiMAX applications. The reduced ground plane aids in achieving a good impedance match, and the proposed structures have additional resonance by the addition of the SRR to the substrate's bottom extremity. The proposed antenna's resonant properties are altered with the addition of the SRR. A study is done on SRR's negative permeability feature. To get the desired outcome, a parametric study of the feed width, slot width, and ground height is conducted.

2 DUAL-BAND SRR INCORPORATED ANTENNA

The most desirable material for antennas is FR4, which has a relative permittivity (r) of 4.4, a loss tangent of 0.02, a thickness of 1.6 millimetres, and dimensions of width by length and by height. A straightforward monopole antenna serves as its primary component. On one side of the substrate lies a simple monopole with a length that, when added together ($L1 + L2$), is equal to $g/2$ of the fundamental frequency (2.8 GHz). Impedance matching is improved by the geometry and size of the ground. Ant 1, Ant 2, Ant 3, and Ant 4 are the four different iterations of the antenna seen in Fig. 1.

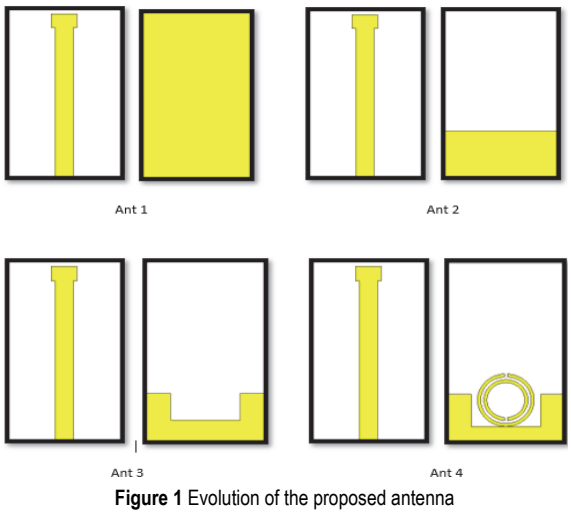

Figure 1 Evolution of the proposed antenna

The parameters of the antenna are shown in Fig. 2.

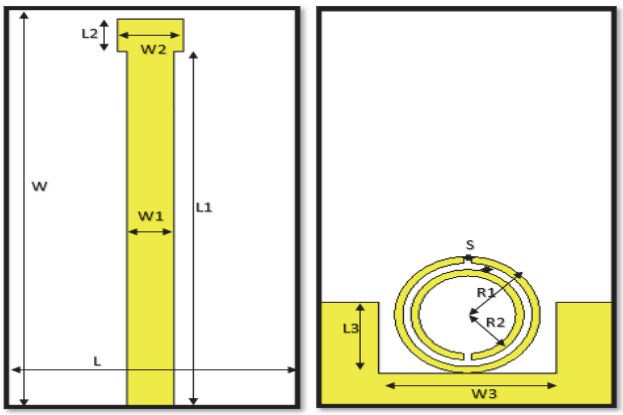

Figure 2 SRR-inspired monopole antenna with its parameter

Table 1 Parameter value of the proposed SRR-inspired monopole

W	*L*	*W*1	*L*1	*W*2	*L*2	*W*3
19	31	3.5	29	4.25	1	11
*L*3	*S*	*R*1	*R*2	*T*	*H*	*Lg*
5.5	0.5	4.5	3.5	0.0035	1.6	8.5

The characteristics of the antenna are detailed in Tab. 1. Due to improper impedance matching, the primary stage of the antenna, which consists of a straight monopole connected to the earth's whole ground, is unable to resonate at the appropriate frequency. The antenna is now resonating at 2.5 GHz but has a very narrow bandwidth as a result of the size reduction that was required for impedance matching with the ground during stage 2 of the antenna growing process. The bandwidth can be increased by cutting a square groove into the defective ground that is 3 millimetres wide and 3 millimetres long. The bandwidth is increased by using antennas in the third stage. The two frequencies are compatible with the antenna with prongs (2.36-2.94 and 5.18-5.73 GHz).

The lack of resonance in the antenna is demonstrated by the ant1 s11 seen in Fig. 3, which is caused by an impedance mismatch.

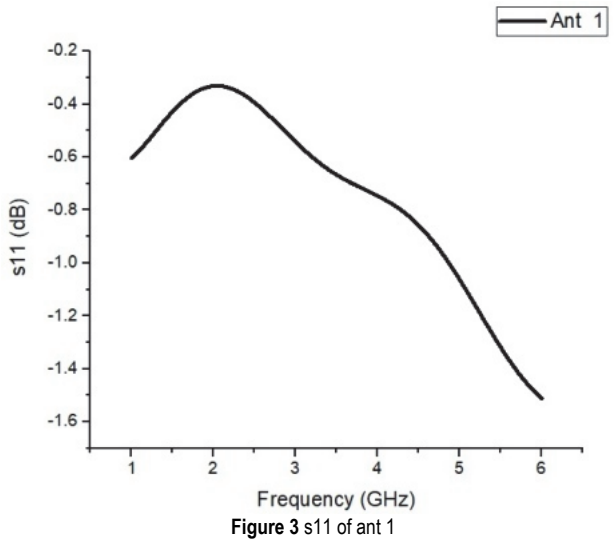

Figure 3 s11 of ant 1

Fig. 4 presents the s11 of antenna 2 which demonstrates impedance matching at 2.5 GHz as a result of the smaller ground area. Fig. 5 shows the s11 of that evolutionary stage, in which the antenna's good bandwidth is attained by exploiting the defective ground structure.

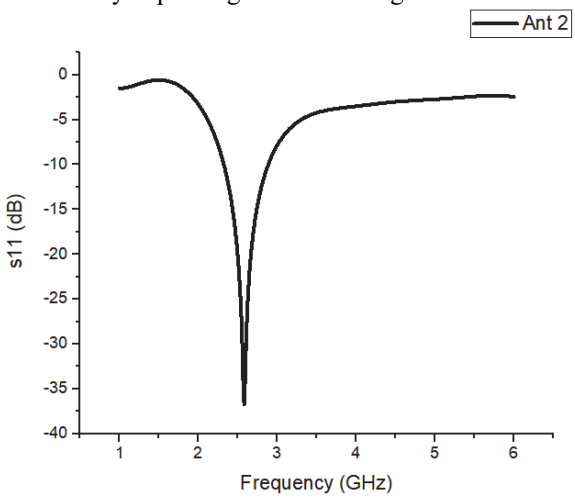

Figure 4 s11 of ant 2

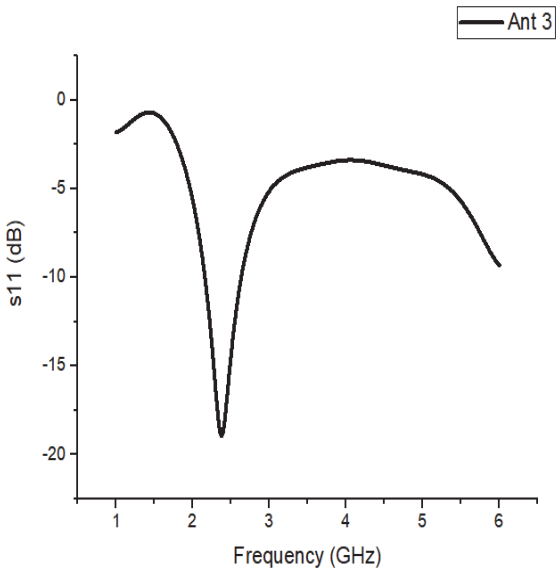

Figure 5 s11 of ant 3

Lastly, the VSWR plot of the antenna and the return loss plot of the proposed antenna are shown in Figs. 6 and 7, respectively. The suggested SRR-based monopole antenna is shown to have dual-band resonance in both graphs. Fig. 8 compares and displays the return loss of the antenna at its various stages.

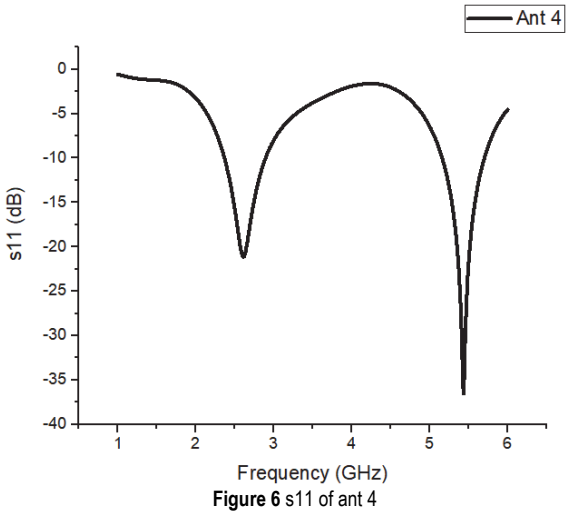

Figure 6 s11 of ant 4

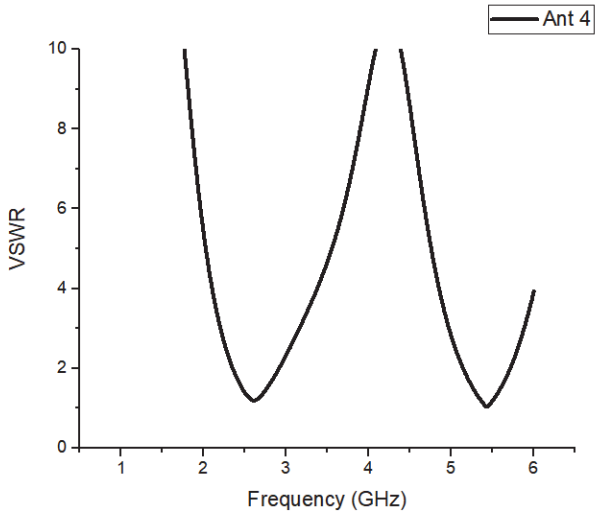

Figure 7 VSWR of ant 4

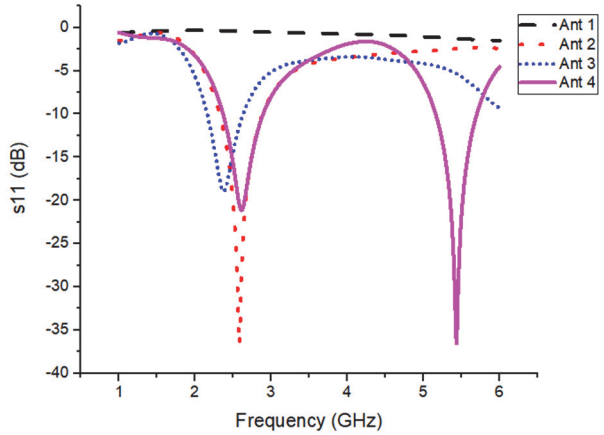

Figure 8 s11 Comparison of the antenna evolved during the SRR-inspired monopole antenna design

3 PARAMETRIC ANALYSIS

In order to optimize the performance of the prosed antenna, the key parameter should have an optimal value. The optimal value of the proposed design is identified with the help of parametric analysis in CST software.

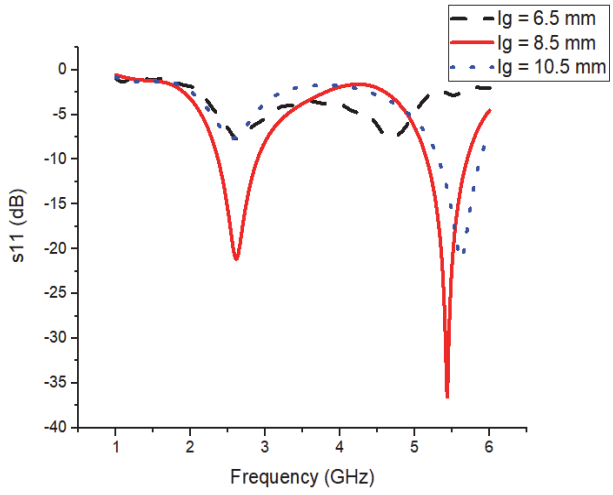

Figure 9 Parametric analysis of ground length

The antenna parameters like ground length and feed width are chosen for the parametric analysis. First the ground length is optimized by increasing the ground length in steps of 2 mm from 6.5 mm to 10.5 mm. The variation in return loss with respect to the ground length is presented in Fig. 9. It shows that at 8.5 mm of ground length the prosed antenna is having good impedance bandwidth in both bands.

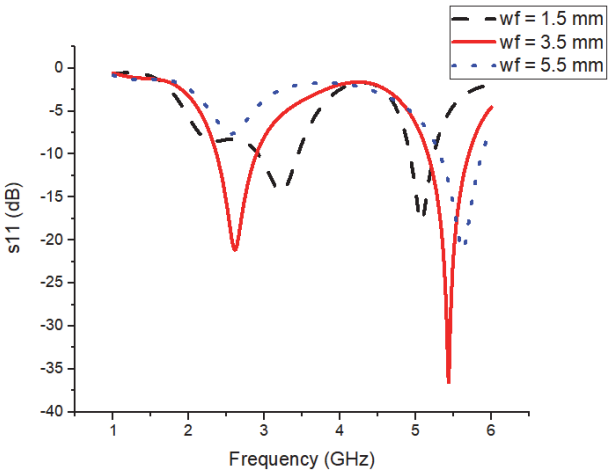

Figure 10 Parametric analysis of feed width

In Fig. 10, the return loss is plotted for various values of feed width. The feed width is increased in steps of 2 mm from 1.5 mm to 5.5 mm. The proposed antenna is exhibiting good impedance bandwidth at both bands when the feed width is 3.5 mm. Then the parameters of the split ring resonator are optimized to have the 5.2 GHz, resonant band. First, the outer ring radius *R*1 is increased in steps of 1 mm from 3.5 mm to 4.5 mm, and the performance variation of return loss is plotted in Fig. 11.

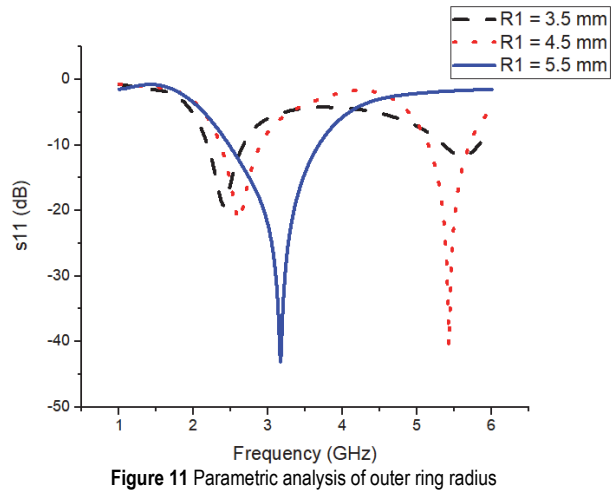

Figure 11 Parametric analysis of outer ring radius

From the figure, the antenna is having good impedance matching at the resonant frequency of 5.2 GHz after the introduction of SRR. Then the inner radius of the SRR R2 is optimized. *R*2 is increased from 2.5 to 4.5 mm in steps of 1 mm. The variation is plotted in Fig. 12, which shows the *R*2 affects both the resonating bands.

The SRR split width is optimized by increasing it in steps of 0.5 mm from 0 mm to 1 mm. The various values of the return loss with respect to the various values of split width are presented in Fig. 13. The antenna with SRR split width of 0.5 mm has good impedance bandwidth as shown

in the figure below. Hence for all the parameters the optimized value is chosen for the final fabrication.

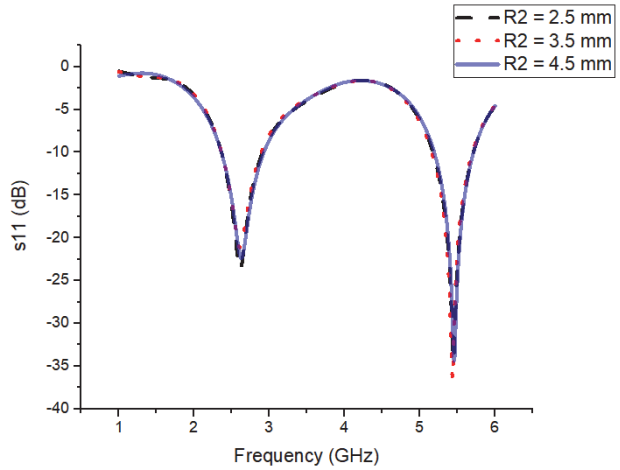

Figure 12 Parametric analysis of inner ring radius

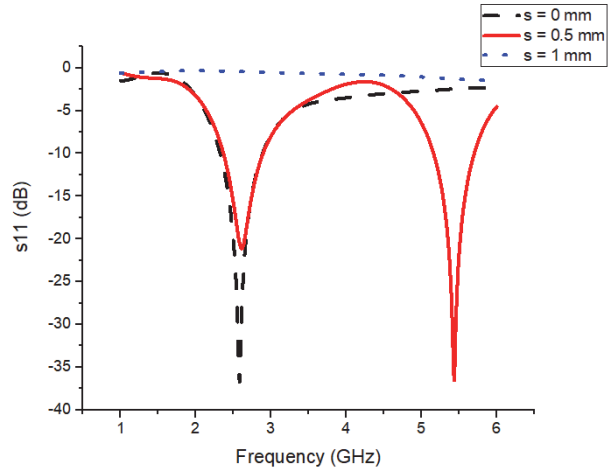

Figure 13 Parametric analysis of SRR split width

4 RESULT AND DISCUSSION

Fig. 14 illustrates a comparison between the surface current distributions of the proposed antenna operating at 2.3 GHz and 5.8 GHz.

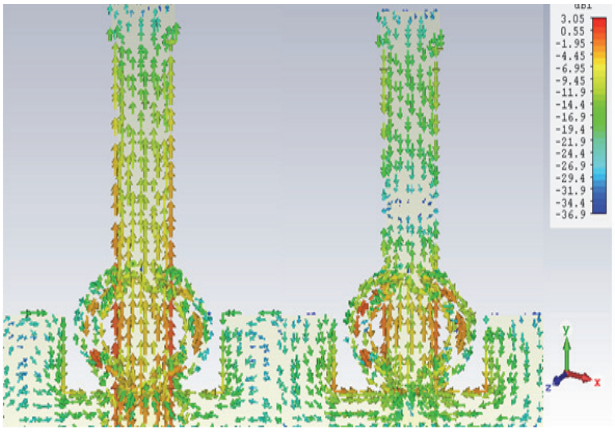

a) 2.3 GHz b) 5.8 GHz

Figure 14 Surface current density

This figure shows that the largest surface current is available around the SRR when operating at 5.8 GHz. This finding makes it clear that the SRR is to blame for the band that is generated at that frequency. The introduction of the SRR leads to a new generation of inductance and capacitance which in turn creates the additional resonance. Fig. 15 depicts the E plane and H plane layout of the suggested structure in its many operational configurations. The radiation pattern in the E plane was omnidirectional due to the fact that it was symmetrical with respect to the vertical axis, but the radiation pattern in the H plane was only bidirectional.

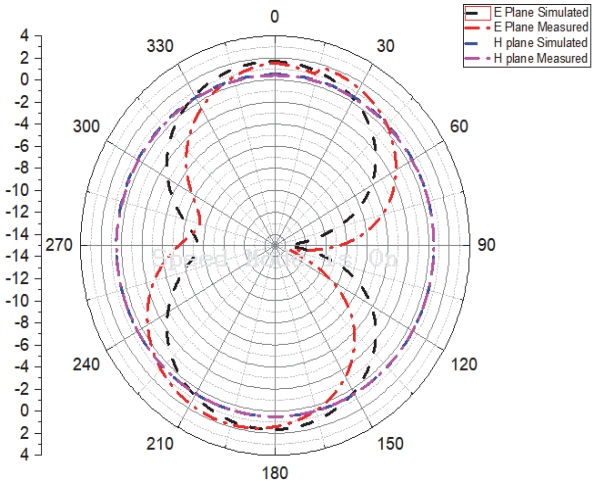

Figure 15a 2.3 GHz E plane and H plane (measured vs simulated)

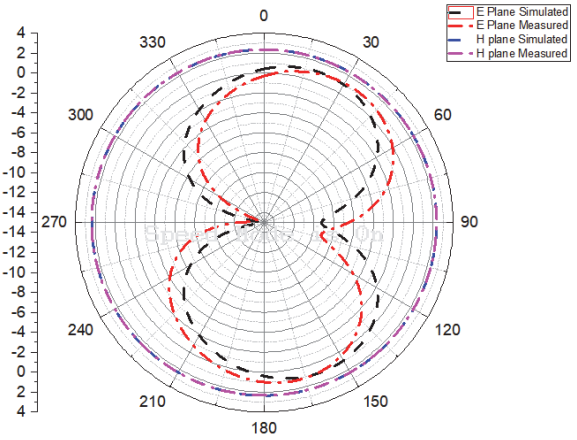

Figure 15b 5.8 GHz E plane and H plane (measured vs simulated)

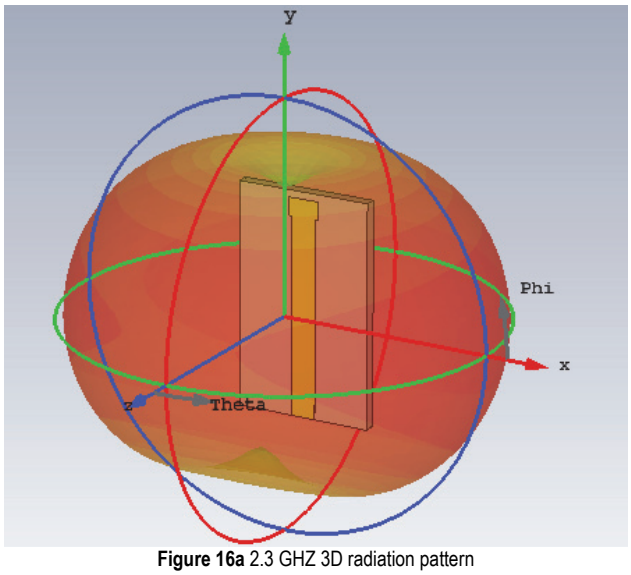

Figure 16a 2.3 GHZ 3D radiation pattern

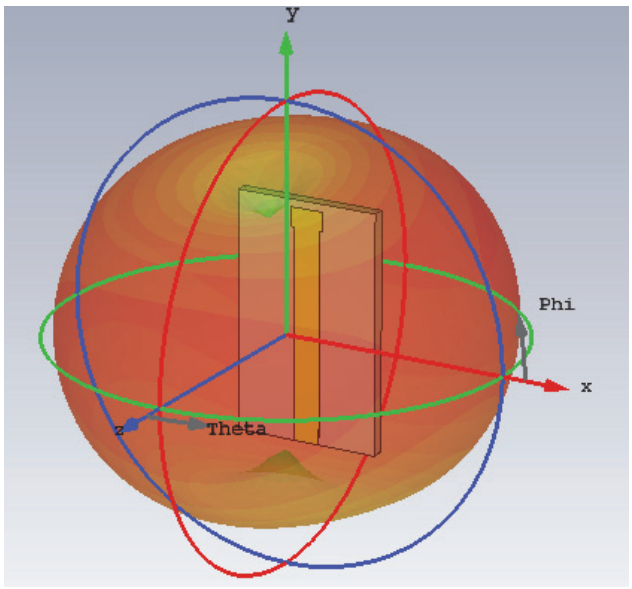

Figure 16b 5.8 GHz 3D radiation pattern

In Fig. 16, the 3-dimensional radiation pattern is presented which is omni-directional in nature. The fabricated antenna which is presented in Fig. 17, is fabricated with the help of photo etching process. The following steps have been adopted for the fabrication of the proposed antenna. The double-sided copper-clad FR4 substrate is cleaned with acetone. The structure is laminated with the photo resist film after dried up. Then the mask which is the negative of the proposed design is attached to the photo resist laminated FR4 substrate and exposed to UV light. Then the substrate is dissolved in sodium carbonate developer solution and etching process using ferric chloride solution. Then the sodium hydroxide is used to remove the harden photo resist to developed the proposed antenna.

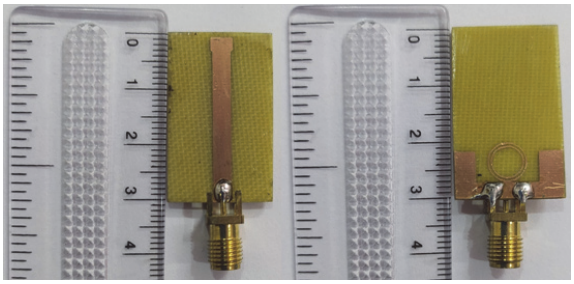

Figure 17 Fabricated antenna

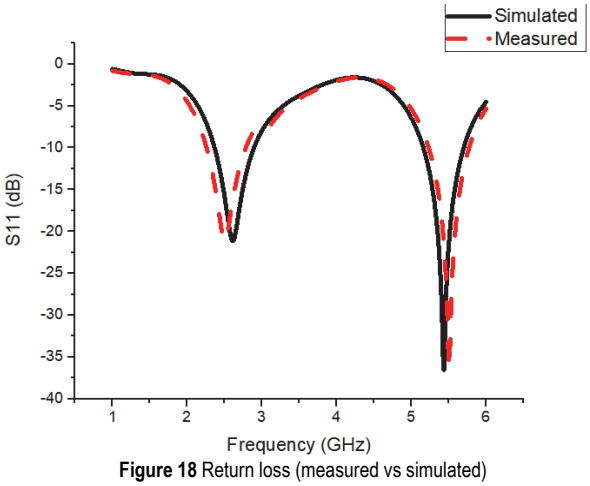

Figure 18 Return loss (measured vs simulated)

In Fig. 18, the return loss measured result is compared with the simulated result, which shows some deviation which is due to measurement and fabrication error. Fig. 19 shows the predicted and actual gain from a simulation. It is easy to see that the proposed design has a gain greater than 1.5 dBi in the usable frequency range. The bandwidth of 580 and 550 MHz is achieved in the above-proposed antenna due to the radiating elements and the inclusion of the SRR near the ground. The SRR and radiating element modes are responsible for the bandwidth achieved.

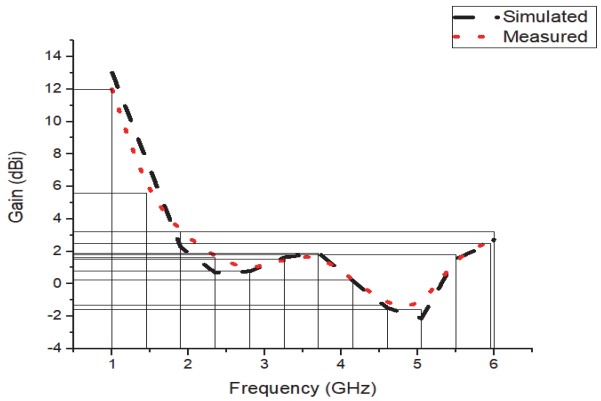

Figure 19 Gain (measured vs simulated)

5 CONCLUSION

We show a monopole antenna with a defective ground structure that was conceptualized with the help of metamaterials. This antenna will be used for the wireless medical device as well as other wireless applications. The results of a CST simulation are displayed here. To create a comprehensive image of the structure, we take into account its return loss, gain, current distribution, and radiation pattern. Because the original design of a basic monopole with the complete ground and no impedance matching did not include a metamaterial at the back of the substrate or a rectangular slit in the ground, dual-band functioning is only achievable because of these two additions. The antenna has been constructed and put through its paces; its tri-band resonance may be found at 2.3 GHz and 5.8 GHz. The results obtained through simulation are equivalent to those obtained from measurements in terms of s11, gain, and directivity, as well as E-plane and H-plane pattern. The framework that has been provided is adaptable enough to work properly in ISM networks, WLAN networks, WiMAX networks, and WIFI networks.

6 REFERENCES

[1] Kunwar, A., Gautam, A. K., & Rambabu, K. (2017). Design of a compact U-shaped slot triple band antenna for WLAN/WiMAX applications. *AEU-International Journal of Electronics and Communications*, *71*, 82-88. https://doi.org/10.1016/J.AEUE.2016.10.013

[2] Amani, N., Kamyab, M., Jafargholi, A., Hosseinbeig, A., & Meiguni, J. S. (2014). Compact tri-band metamaterial-inspired antenna based on CRLH resonant structures. *Electronics Letters*, *12*, 847-848. https://doi.org/10.1049/el.2014.0875

[3] Rajak, N. & Chattoraj, N. (2017). A bandwidth-enhanced metasurface antenna for wireless applications. *Microwave and Optical Technology Letters*, *59*, 2575-2580.

https://doi.org/10.1002/mop.30769
[4] George, J., Aanandan, C. K., Mohanan, P., Nair, K. G., Sreemoolanathan, H., & Sebastian, M. T. (1998). Dielectric resonator loaded microstrip antenna for enhanced impedance bandwidth and efficiency. *Microwave and Optical Technology Letters*, *17*, 205-207.
[5] Wu, W., Yuan, B., Guan, B., & Xiang, T. (2017). A bandwidth enhancement for metamaterial microstrip antenna. *Microwave and Optical Technology Letters*, *59*, 3076-3082. https://doi.org/10.1002/mop.30872
[6] Razali, A. R. & Bialkowski, M. E. (2012). Dual-band slim inverted-F antenna with enhanced operational bandwidth. *Microwave and Optical Technology Letters*, *54*, 684-689. https://doi.org/10.1002/mop.26643
[7] Peng, L., Mao, J. Y., Li, X. F., Jiang, X., & Ruan, C. L. (2017). Bandwidth enhancement of microstrip antenna loaded by parasitic zeroth-order resonators. *Microwave and Optical Technology Letters*, *59*, 1096-1100. https://doi.org/10.1002/mop.30471
[8] Fan, S. T., Yin, Y. Z., Hu, W., Li, B., & Yang, J. H. (2012). Bandwidth enhancement of a printed dipole antenna for wideband applications. *Microwave and Optical Technology Letters*, *54*, 1585-1590. https://doi.org/10.1002/mop.26883
[9] Reddy, S. V., Sarkar, D., Saurav, K., & Srivastava, K. V. (2015). LC resonator loaded bandwidth-enhanced tri-band planar inverted-F antenna. *Microwave and Optical Technology Letters*, *57*, 1879-1883. https://doi.org/10.1002/mop.29211
[10] Rajeshkumar, V. & Raghavan, S. (2015). Bandwidth-enhanced compact fractal antenna for UWB applications with 5-6 GHz band rejection. *Microwave and Optical Technology Letters*, *57*, 607-613. https://doi.org/10.1002/mop.28913
[11] Luo, Y., Chu, Q. X., & Bornemann, J. (2017). A Differential fed YagUda antenna with enhanced bandwidth via addition of parasitic resonator. *Microwave and Optical Technology Letters*, *59*, 156-159. https://doi.org/10.1002/mop.30253
[12] Mehdipour, A., Denidni, T. A., & Sebak, A. R. (2014). Multiband miniaturized antenna loaded by ZOR and CSRR metamaterial structures with monopolar radiation pattern. *IEEE Transactions on Antennas and Propagation*, *62*(2), 555-562. https://doi.org/10.1109/TAP.2013.2290791
[13] Yoo, M. a& Lim, S. (2013). SRR and CSRR loaded ultra-wideband (UWB) antenna with tri-band notch capability. *Journal of electromagnetic waves and applications*, *27*, 2190-2197. https://doi.org/10.1080/09205071.2013.837013
[14] Xu, H. X., Wang, G. M., Zhang, C. X., & Peng, Q. (2011). Hilbert shaped complementary single split ring resonator and low-pass filter with ultra-wide stop band, excellent selectivity and low insertion loss. *AEU International journal for Electronics and Communications*, *65*, 901-905. https://doi.org/10.1016/j.aeue.2011.02.012
[15] Hamidreza, M. T., Ramesh, A., & Mohsen, N. (2016). A cavity backed antenna loaded with complimentary split ring resonators. *AEU International journal for Electronics and Communications*, *70*, 928-935. https://doi.org/10.1016/j.aeue.2016.04.010
[16] Phani Kumar, K. V. & Karthikeyan, S. S. (2015). Wideband three section branch line coupler using triple open complementary split ring resonator and open stubs. *AEU International journal for Electronics and Communications*, *69*, 1412-1416. https://doi.org/10.1016/j.aeue.2015.06.003
[17] Caloz, C. & Itoh, T., (2006). *Electromagnetic metamaterials Transmission line theory and microwave applications*. John Wiley & Sons Inc. Publication. https://doi.org/10.1002/0471754323
[18] Elavarasi, C. & Shanmuganantham, T. (2016). SRR loaded CPW fed multiple band rose flower shaped fractal antenna. *Microwave and Optical Technology Letters*, *58*, 1720-1724. https://doi.org/10.1002/mop.30609
[19] Asad, M. J., Shafique, M. F., & Khan, S. A. (2017). Performance restoration of dielectric embedded antennas using omega like complementary split ring resonators. *Microwave and Optical Technology Letters*, *59*(2), 357-362.
[20] Falcone, F., Illescas, J., Jarauta, E., Estevez, A., & Marcotegui, J. A. (2013). Analysis of stripline configurations loaded with complementary split ring resonators. *Microwave and Optical Technology Letters*, *55*, 1250-1254. https://doi.org/10.1002/mop.27569
[21] Boopathi Rani, R. & Pandey, S. K. (2017). Metamaterial inspired printed UWB antenna for short range RADAR applications. *Microwave and Optical Technology Letters*, *59*, 1600-1604. https://doi.org/10.1002/mop.30590
[22] Choudhury, S. & Mohan, A., (2017). Miniaturized Sierpinski fractal loaded QMSIW antenna with CSRR in ground plane for WLAN applications. *Microwave and Optical Technology Letters*, *59*, 1294-1295. https://doi.org/10.1002/mop.30528
[23] Boopathi Rani, R. & Pandey, S. K. (2017). A CPW fed circular patch antenna inspired by reduced ground plane and CSRR slot for UWB applications with notch band. *Microwave and Optical Technology Letters*, *59*, 745-749. https://doi.org/10.1002/mop.30386
[24] Sam, P. J. C. & Gunavathi, N. (2020). A tri-band monopole antenna loaded with circular electric-inductive-capacitive metamaterial resonator for wireless application. *Applied Physics A*, *126*(10). https://doi.org/10.1007/s00339-020-03952-1
[25] Sam, P. J. C. & Gunavathi, N. (2021). Octa-Band Metamaterial Inspired Multiband Monopole Antenna for Wireless Application. *Progress in Electromagnetics Research C*, *113*, 97-110. https://doi.org/10.2528/PIERC21041102
[26] Orhan, A. & Mesud, K. (2022). The Effect of the Co-Planar Structure on HPBW and the Directional Gain at the Square Patch Antenna around ISM 2450 MHz, *Technical Gazette*, *29*(4), 1120-1125. https://doi.org/10.17559/TV-20190423010908

Contact information:

Ms. Roja GANESAN, Lecturer
Dept of Electronics and Communication Engineering,
Periyar Centenary Polytechnic College, Vallam, Thanjavur

Dr. Maheswara Venkatesh PANCHAVARNAM, Assistant Professor
(Corresponding author)
Dept of Electronics and Communication Engineering,
University College of Engineering, BIT Campus, Anna University, Tiruchirapalli
E-mail: maheshwaravenkatesh@gmail.com

Dr. Jayasankar THANGAIYAN, Assistant Professor
Dept of Electronics and Communication Engineering,
University College of Engineering, BIT Campus, Anna University, Tiruchirapalli